2006 Earth Science Technology Conference
University of Maryland Inn and Conference Center
June 27, 2006

Development of an Agile Digital Detector for RFI Detection and Mitigation on Spaceborne Radiometers

Chris Ruf, Sid Misra, April Warnock, Chip Wineland, Steve Gross & Roger De Roo
Dept. of Atmospheric, Oceanic and Space Sciences, University of Michigan
Joel Johnson, Noppasin Niamsuwan & Baris Guner
Dept. of Electrical Engineering, Ohio State University
Jeff Piepmeier, Joe Knuble, Priscilla Mohammed, Brian LaRocque & Jared Lucey
NASA Goddard Space Flight Center

Project Objectives

- **Technical Objectives**
  - Design, develop and field test three candidate RFI mitigation detectors
  - Develop RFI mitigation algorithms and characterize their performance
    - Analytical performance models
    - Empirical field testing
  - Assess space qualified parts options and develop a candidate point design
- **Technology Infusion**
  - Integrate RFI mitigation detectors with established ground based and airborne microwave radiometers
  - Demonstrate capabilities to the science community
  - Operate successfully in a relevant (*i.e.* TRL-6) environment

Project Schedule

- Year 1 (7/05-6/06)
  - Prototype RFI Detector development
  - Ground based & airborne campaigns
- Year 2 (7/06-6/07)
  - Campaign data analysis
  - Define flight detector requirements
  - Assess trade space of flight qualifiable options
- Year 3 (7/07-6/08)
  - Advanced detection and mitigation algorithm development
  - Spaceflight detector design

Introduction

- RFI can cause significant errors in science data
  - Soil moisture measurements over land
  - C-Band and X-band ocean measurements near land
- High levels of RFI are relatively easy to detect and mitigate against using analog parallel subband filter approach
- Low levels of RFI present more difficulty
  - Low integrated energy looks like science signal
  - High-power, short-duration → low integrated energy
  - Many sources (*e.g*. air-traffic control radars) match this profile
- Digital signal processing approach
  - Based on statistical properties of natural emission vs. man-made interference

Theory of Operation

- Desired radiometric (science) signals generated by thermal noise
  - Amplitude of electric field has a gaussian (bell-curve) probability density function (PDF)
- RFI is man-made
  - PDFs will often be non-Gaussian
- Exploiting this distinction is the basis of the Agile Digital Detector (ADD)

Approaches to Detecting RFI

1. **Time domain – look for pulses**
2. **Frequency domain – look for carrier frequencies**
3. **Amplitude domain – look for non-thermal distribution**

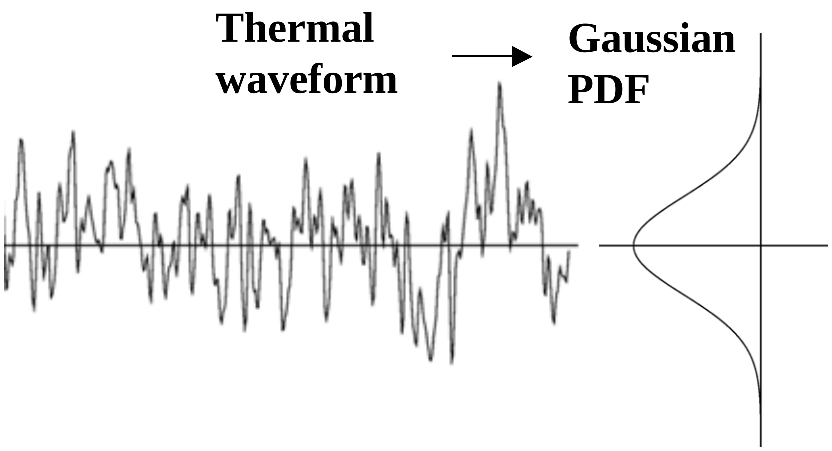

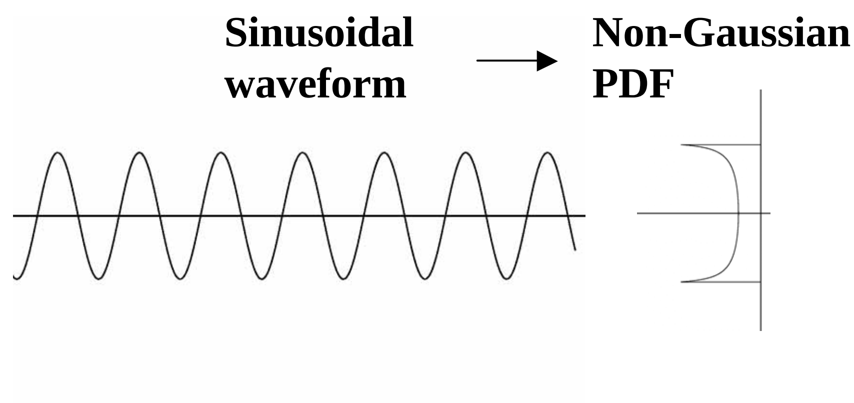

RFI Detection Using Higher Order Moments

- The kurtosis of a random variable, *x*, is defined as

$$k = \frac{<(x-<x>)^4>}{<(x-<x>)^2>^2}$$

- k=3 for a gaussian distributed r.v., independent of σ_x^2
  (*i.e.* k=3 for natural thermal noise, independent of brightness temperature)
- The standard deviation of an estimate of k after a finite integration time is

$$\Delta k = \sqrt{\frac{24}{B\tau}}$$

- For prototype radiometer operation (B=3 MHz & τ=0.3 s), Δk = 0.005
- RFI Detection Flag if |k – 3| > 3Δk

Block Diagram for L-Band ADD (L-ADD)

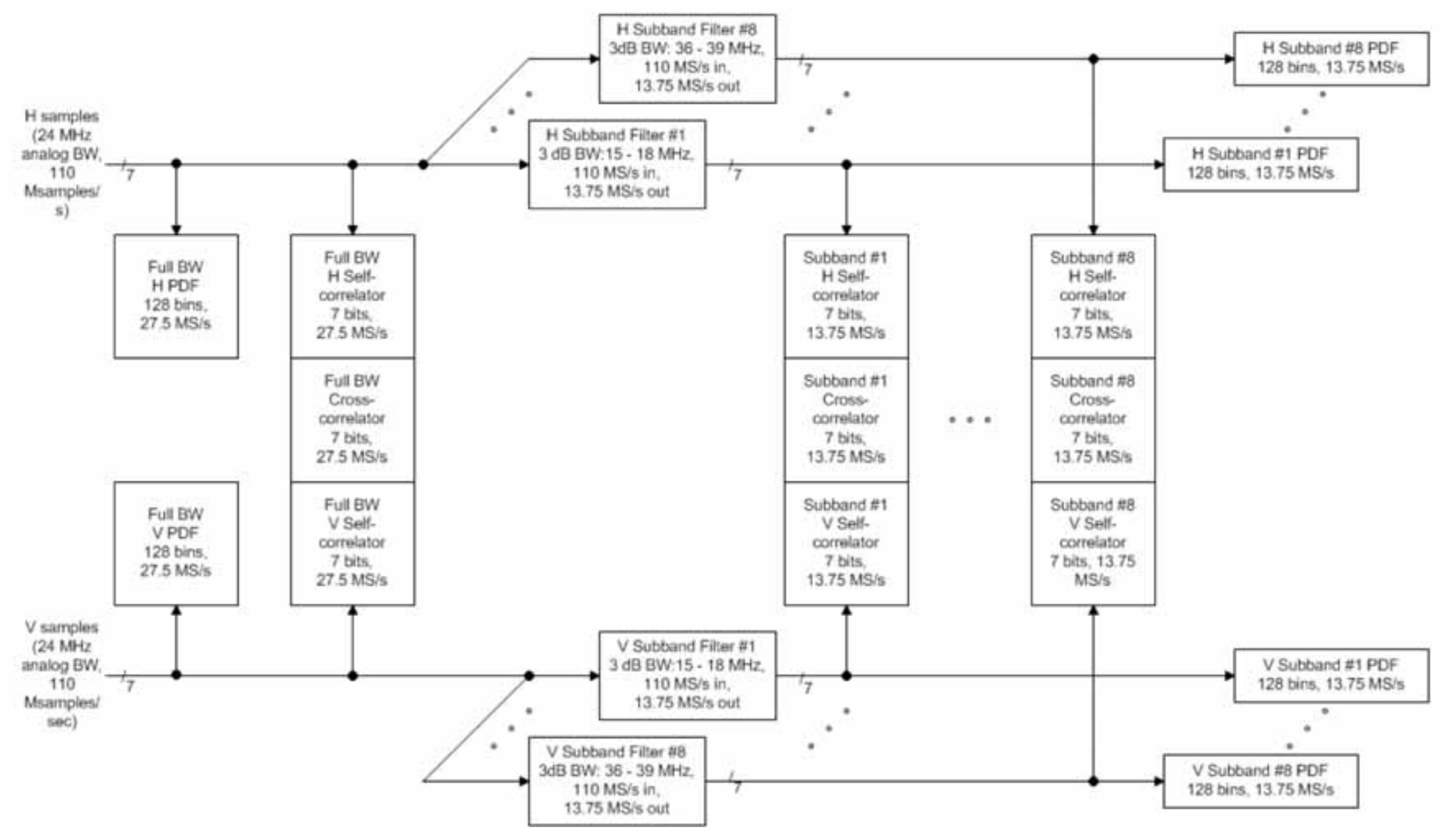

Outdoor Sky Cal with sinusoidal RFI
8 Subband Probability Density Functions

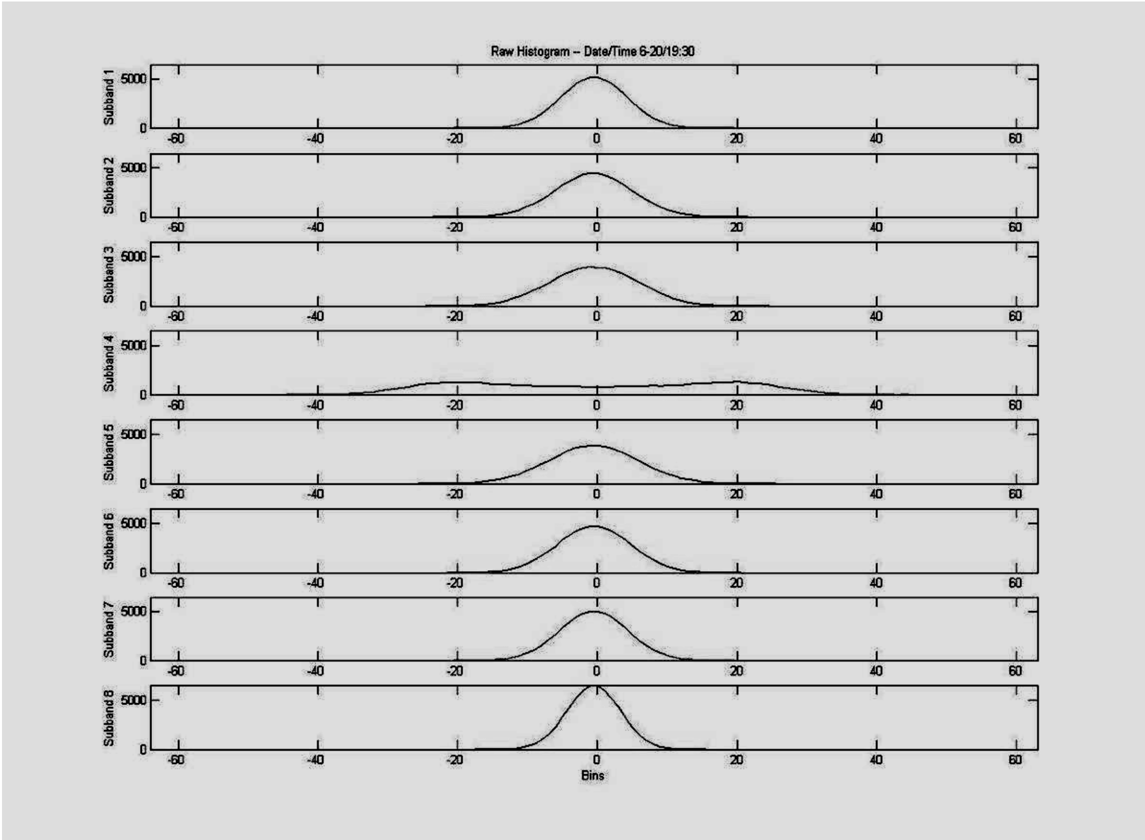

- T_B = 40 K plus ~260 K sine wave injected into subband 5

Experimental Verification – Laboratory Bench Testing

- Use LN_2 cooled blackbody termination
  - 122 K T_B
- Inject pulsed 1412 MHz sine wave
  - 13 K effective ΔT_B
- Normalized moment ratio increased from 1.000 to 2.347

Subband Number (RF Passband, MHz)	Brightness Temperature (K)	Normalized Moment Ratio
#1 (1401.5-1404.5)	121.39 ± 0.34	1.0003 ± 0.002
#2 (1404.5-1407.5)	122.30 ± 0.37	1.0004 ± 0.002
#3 (1407.5-1410.5)	122.86 ± 0.32	1.0066 ± 0.002
#4 (1410.5-1413.5)	135.48 ± 0.33	2.3466 ± 0.025
#5 (1413.5-1416.5)	123.91 ± 0.36	1.0078 ± 0.003
#6 (1416.5-1419.5)	122.27 ± 0.26	1.0001 ± 0.002
#7 (1419.5-1422.5)	122.64 ± 0.47	1.0010 ± 0.003
#8 (1422.5-1425.5)	122.55 ± 0.29	1.0005 ± 0.002

Summary of Field Campaigns

- U-M, OSU & GSFC RFI detectors installed in ground based L-Band radiometer
  - May ’05: Artificial radar pulses added to LN_2 BB Load
  - Jun ’05: Field deployment near ARSR-1 air traffic control radar
  - First refereed publication (IEEE TGRS, **44**(3), 694-706, 2006)
- U-M & OSU RFI detectors installed in NOAA/ETL PSR C-Band Stepped LO channel
  - Aug ’05: Airborne flight over Houston/Dallas/San Antonio/Gulf of Mexico
  - Data analysis in progress
- U-M, OSU & GSFC RFI detectors installed in JPL PALS L-Band radiometer (Aquarius testbed)
  - Data analysis just beginning

Detroit ARSR-1 Field Deployment

- Integrated with truck mounted fully polarimetric L-Band radiometer
- Deployed June 2005 near Detroit International Airport ARSR-1 air traffic control radar site

Kurtosis Time Series During ARSR-1 Deployment

- 6-Hz azimuth scan rate of radar clearly visible in sub-band #1
- Sub-bands #4 and #5 moment ratio considerably greater than unity
- Sub-bands #6-8 are clean so RFI can be mitigated

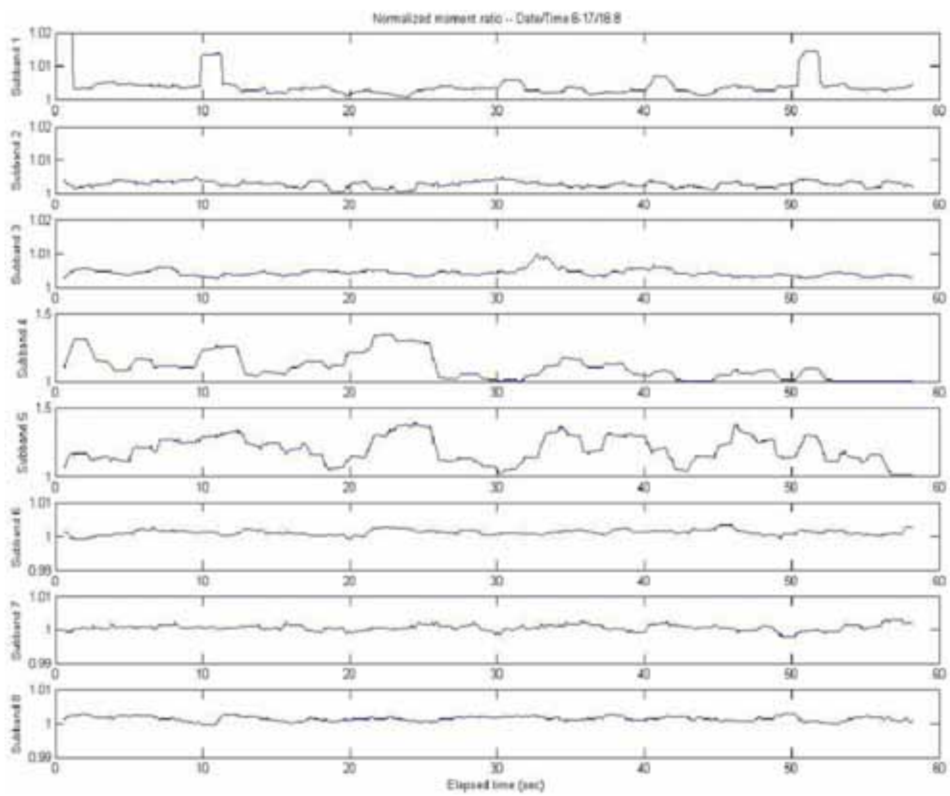

60s time series of RFI-corrected T_B Near ARSR-1

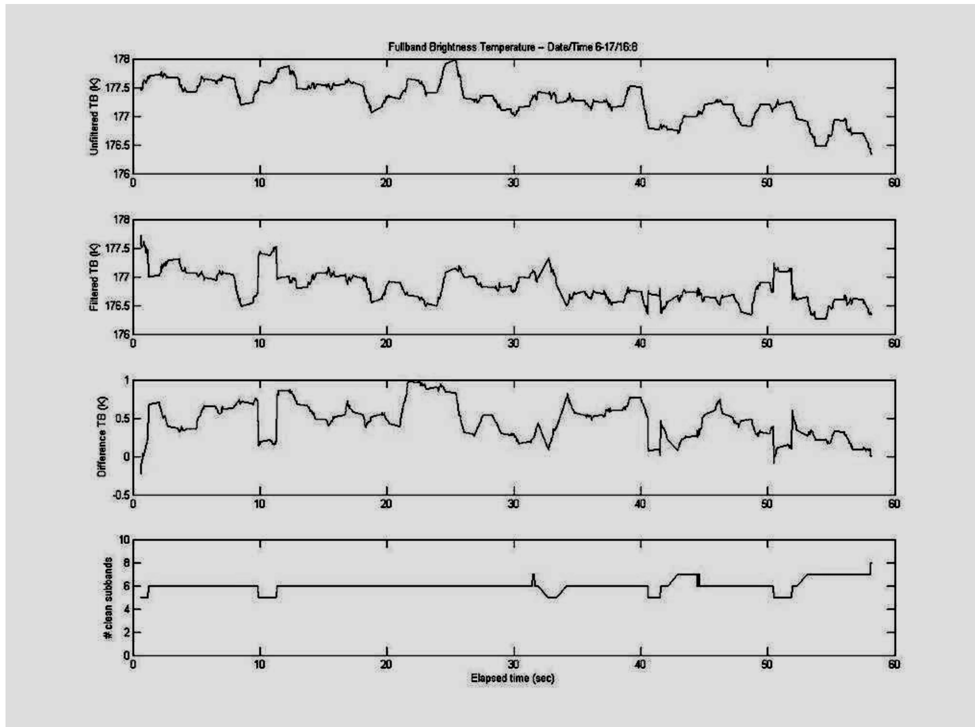

- Row 1: T_B using all 8 subbands
- Row 2: T_B using only subbands with normalized kurtosis within 3σ of 1.000
- Row 3: T_B difference between rows 1&2 (RFI level of 0-1K)
- Row 4: # of RFI-free subbands

C-Band Field Deployment – with NOAA/ETL PSR

- Operated on WB-57 over Texas, 25 August 2005

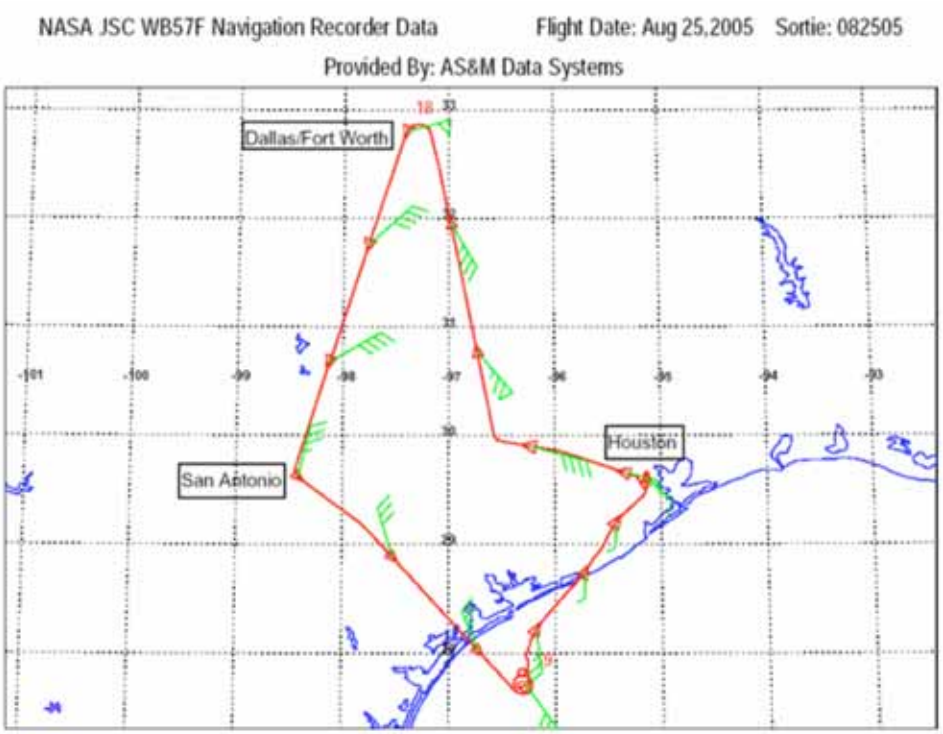

Example of PSR Flight Data
Kurtosis and 2nd Moment Spectra

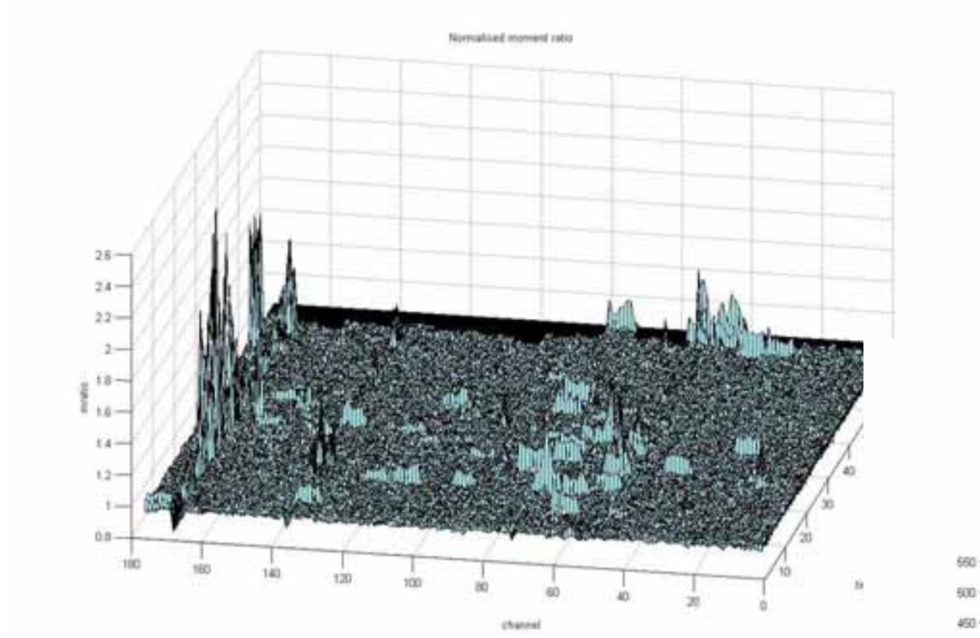

- **Kurtosis (left) and 2nd moment (below) 5.5-7.5 GHz spectra v. time over Dallas Metro area**

- ch = 50-80 (~6 GHz), intermittent times
  - Strong non-gaussian kurtosis
  - Strong, correlated effect on T_B
- ch = 170-180 (~7.5 GHz), t = 0-60s
  - Strong non-gaussian kurtosis
  - Not so noticeable effect on T_B

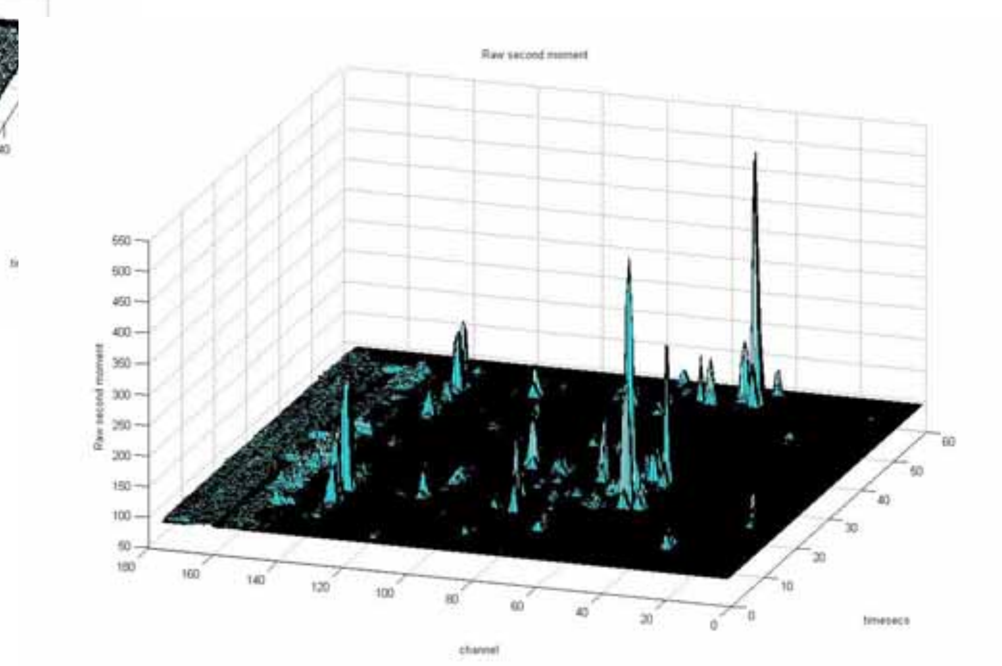

Closer Look at PSR Flight Data – RFI with Weak ΔTB

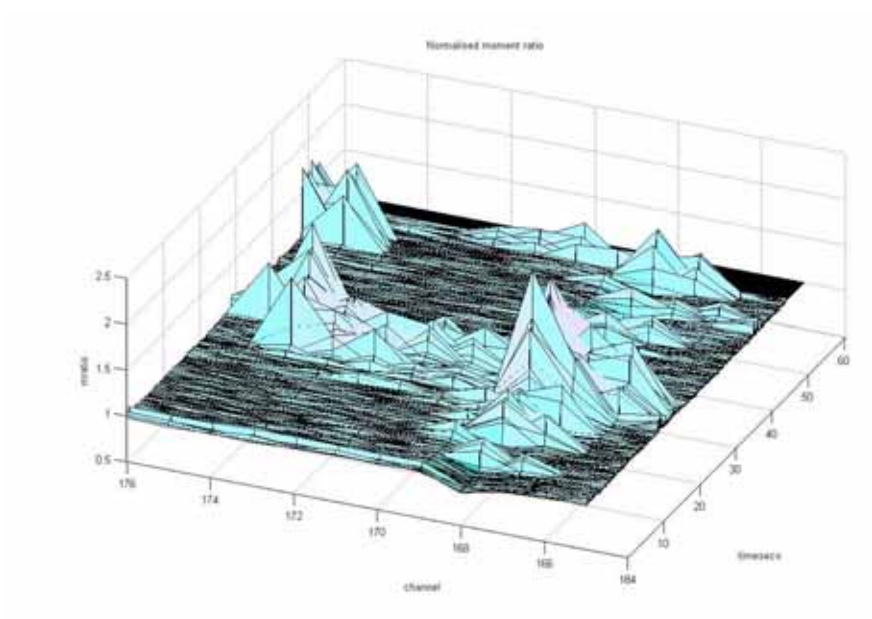

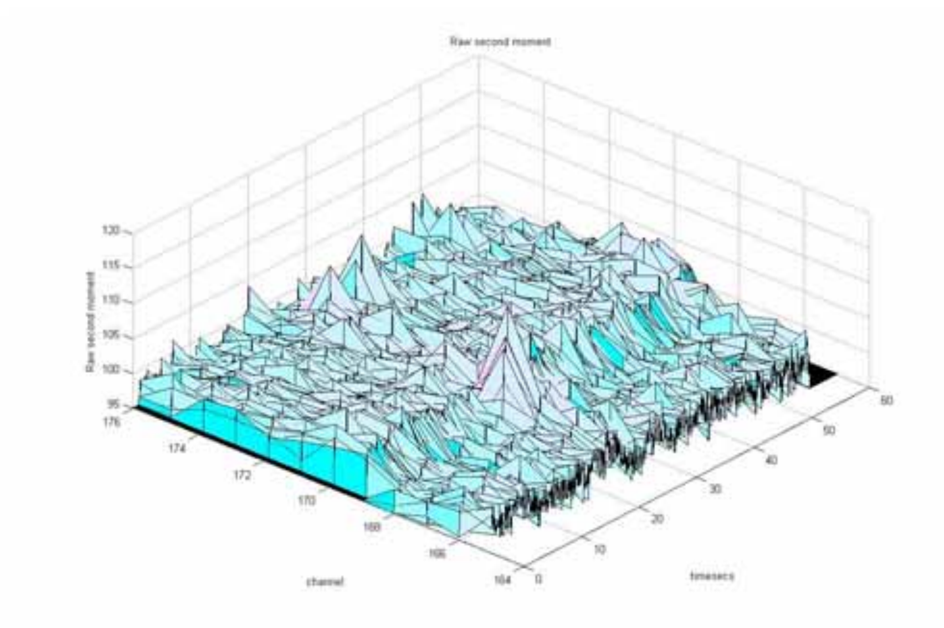

Kurtosis (left) and 2nd moment (right) spectra near 7.5 GHz vs. time over Dallas Metro area.

Regions of significant non-gaussian kurtosis are not accompanied by large spikes in power, implying that the interference is at or near the noise floor of square law detection.

JPL PALS ADD Field Deployment

- Operated at JPL (May 2006)
  - Integrated with PALS radiometer to perform RFI mitigation

Experimental Results – P/D-ADD Field Deployment

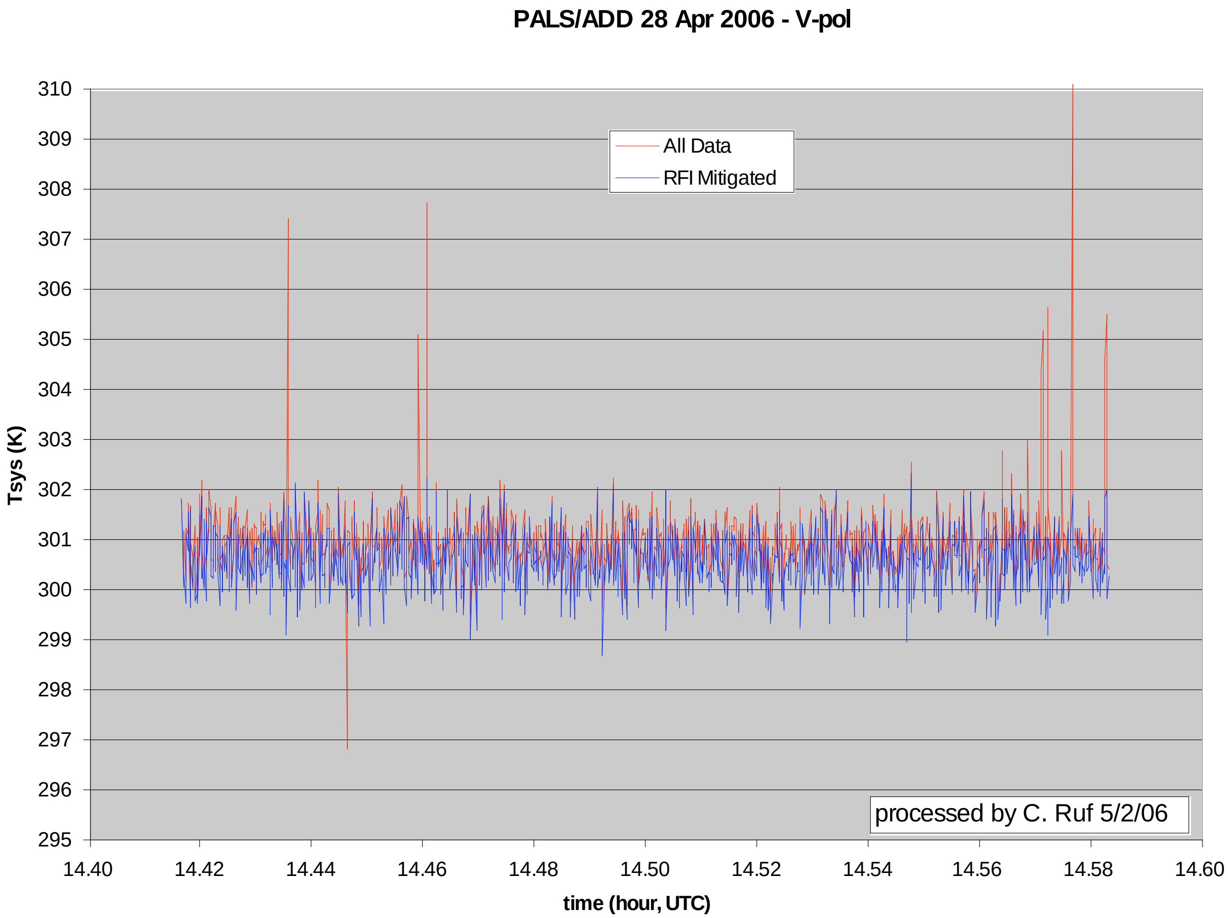

- Mitigation of severe RFI problem on lab at JPL Bldg. 168

False Alarm Rate and Probability of Detection of Pulsed Sinusoidal RFI

- For RFI power level at brightness temperature equivalent to 2NEΔT, detection threshold can be set to give:
  - 90% probability of detection
  - 3% false alarm rate
- 0.1% duty cycle case corresponds to ARSR-1 operating mode
- Higher duty cycle reduces detectability

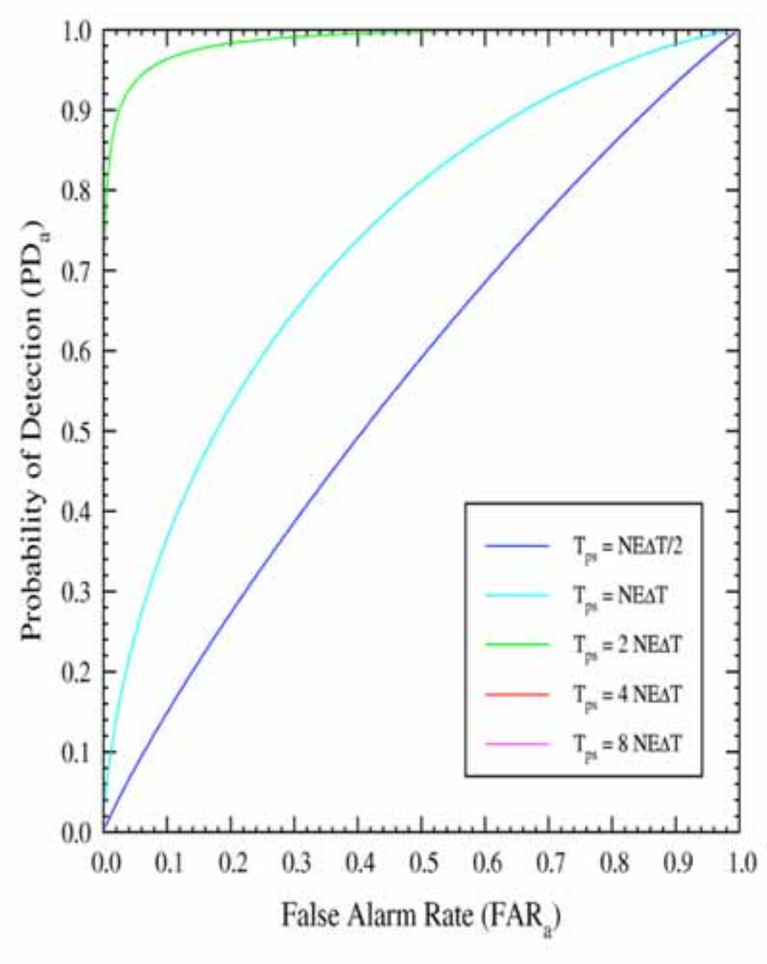

RFI Signal Characterization Capabilities by UM, OSU and GSFC Research Groups

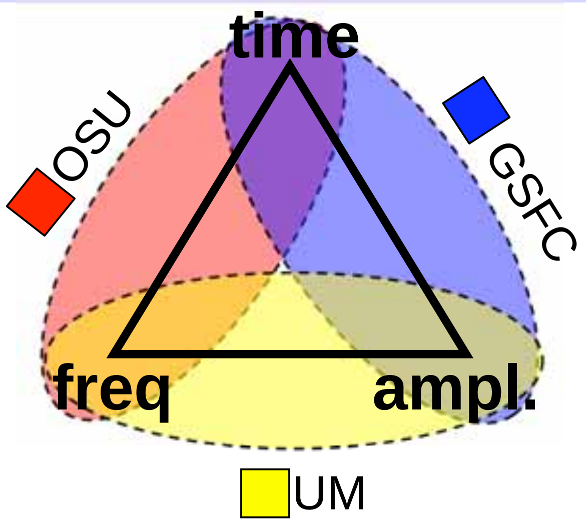

- Methods of RFI characterization used by each research group are complimentary and cross-checking
  - **University of Michigan (UM): generalized amplitude statistics and moderate frequency resolution**
  - **Ohio State University (OSU): ultrafine frequency resolution and fine time resolution**
  - **Goddard Space Flight Center (GSFC): ultrafine time resolution and 2&4 moment amplitude statistics**
- Regions of coverage by each group in (time, frequency, amplitude statistics) signal characterization space are illustrated below

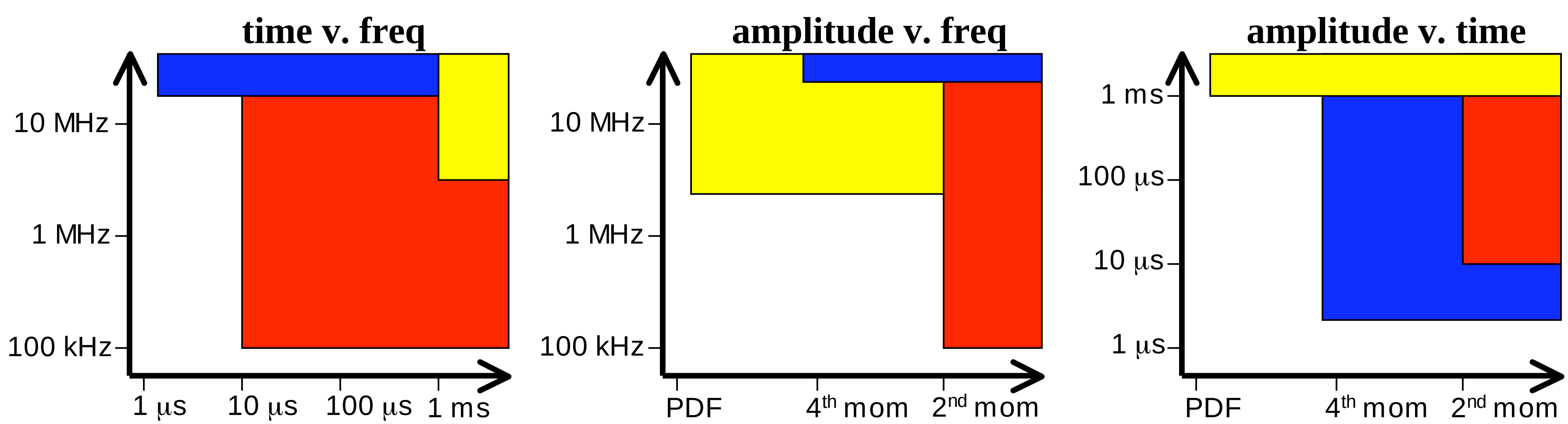

OSU L-band Interference Suppressing Radiometer

- Two 200 MSPS, 10 bit ADC's: can sample either a 100 MHz channel or 2 pols at 50 MHz each, real-time "asynchronous pulse blanking" (APB) algorithm

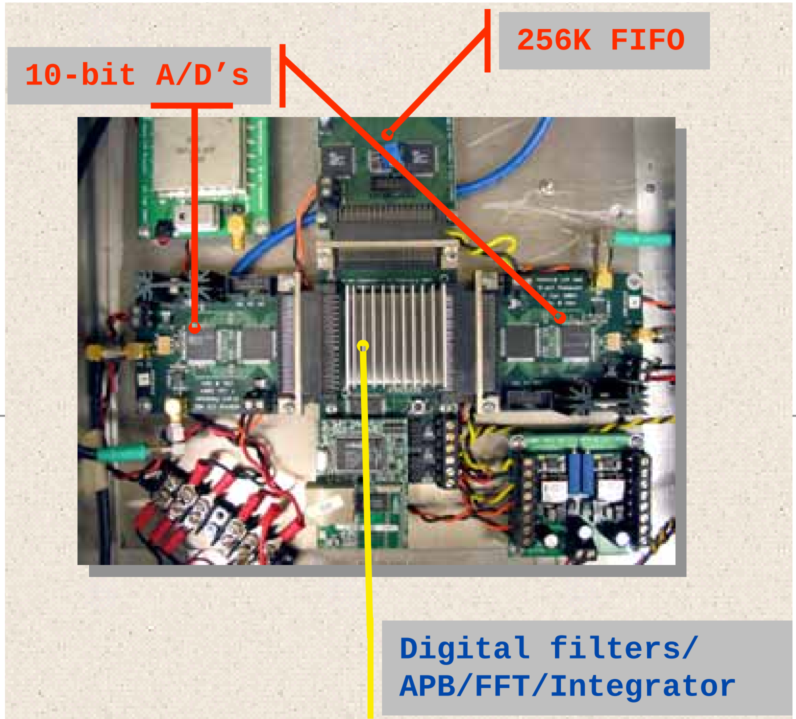

Real-time removal of pulsed interference

- Su '05 Canton campaign results

WB-57F Texas RFI Flight on 25 August 2005

- PSR/C, CISR, and CADD sensors
- Datasets can be intercompared to assess performance
- CISR provides highest spectral resolution

NASA WB-57F

Flight Plan

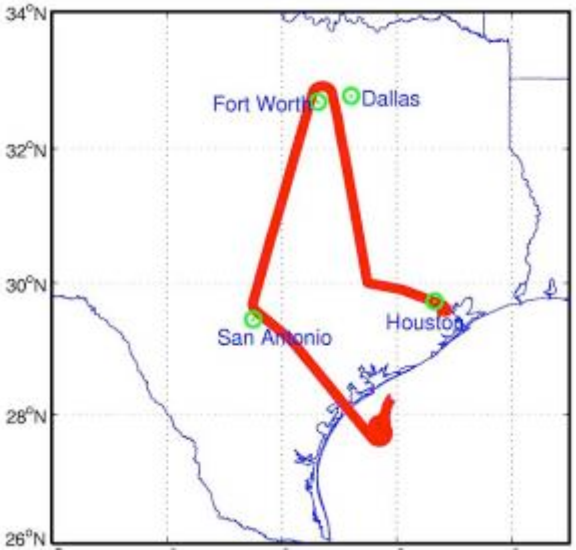

Sample WB-57 OSU CISR Data: 17:55-17:59 UTC

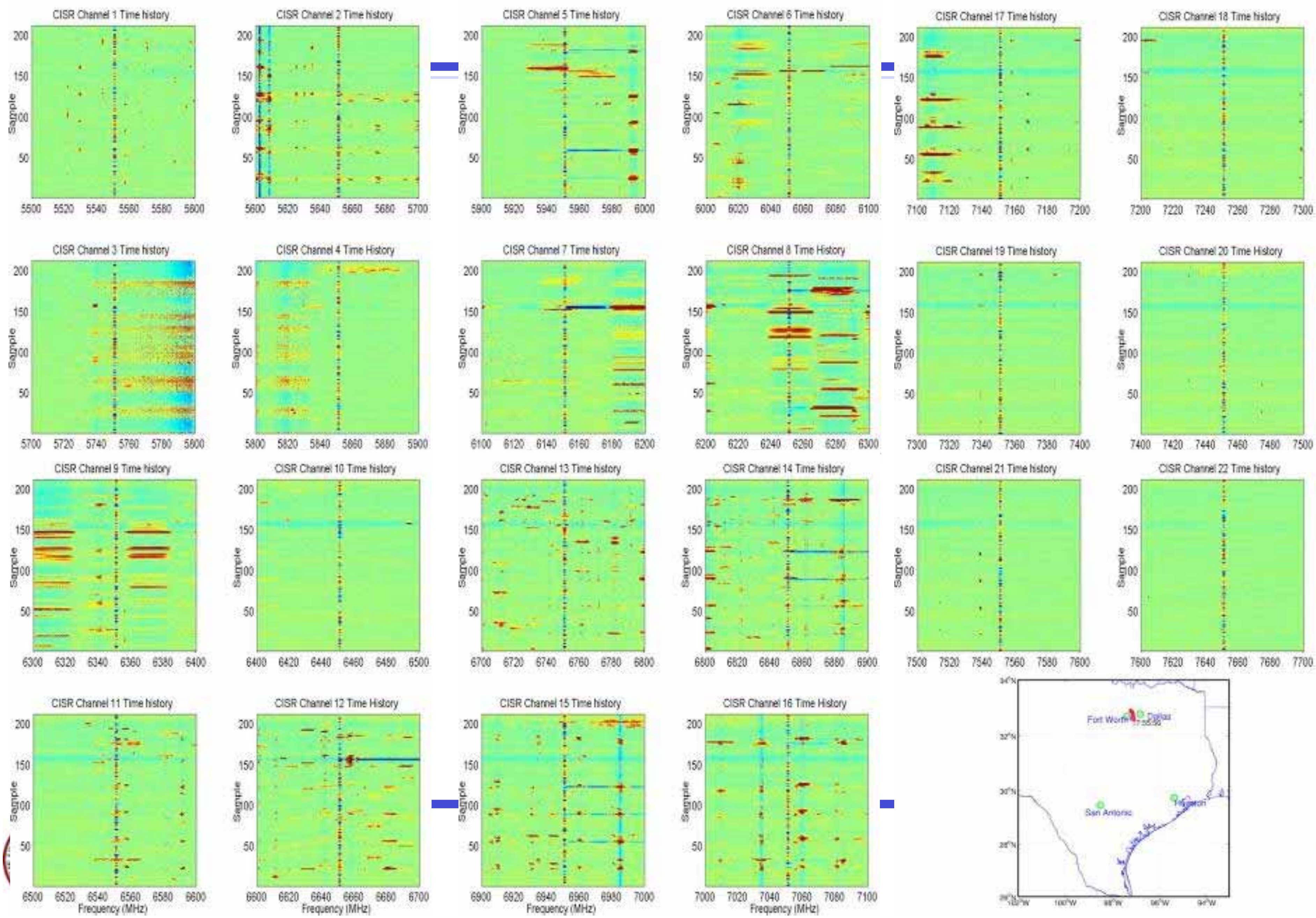

GSFC Contributions

- Developed high-rate (500-kHz) sampling analog back-end
- Standard power detection + pseudo-fourth moment detector
- Primary goals:
  - Risk-reduction exercise (analog vs. digital)
  - Assess performance of post-processing pulse blanking for consideration in HYDROS design
  - Assess implementation in an analog back-end
  - Assess feasibility of analog fourth-moment detector

GSFC Analog Backend

- "Double-detector" architecture
  - Second moment from first detector – conventional power
  - Pseudo-fourth central-moment from second detector
- High-speed sampling and recording
  - 125 kHz video bandwidth on each detector
  - 500 kHz simultaneous sampling streamed to harddisk
  - GPS time-stamping on each file

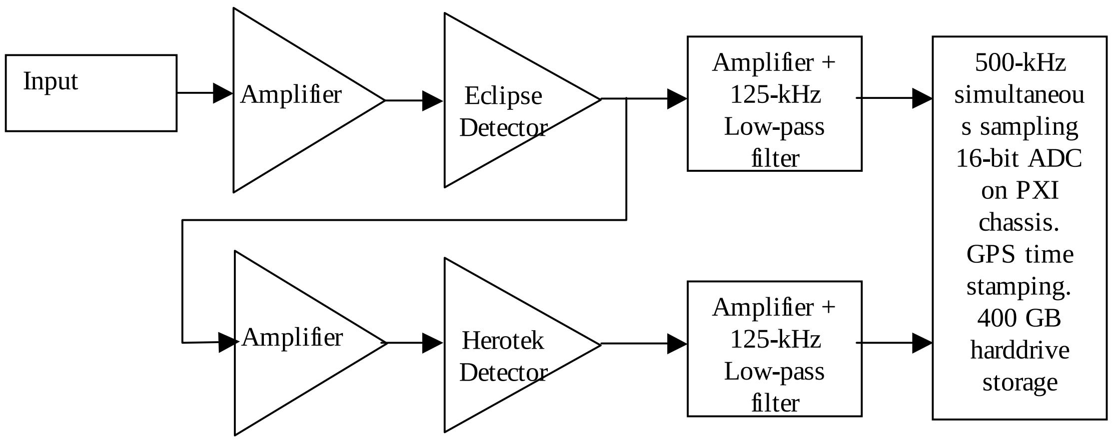

GSFC Analog Double Detector Hardware

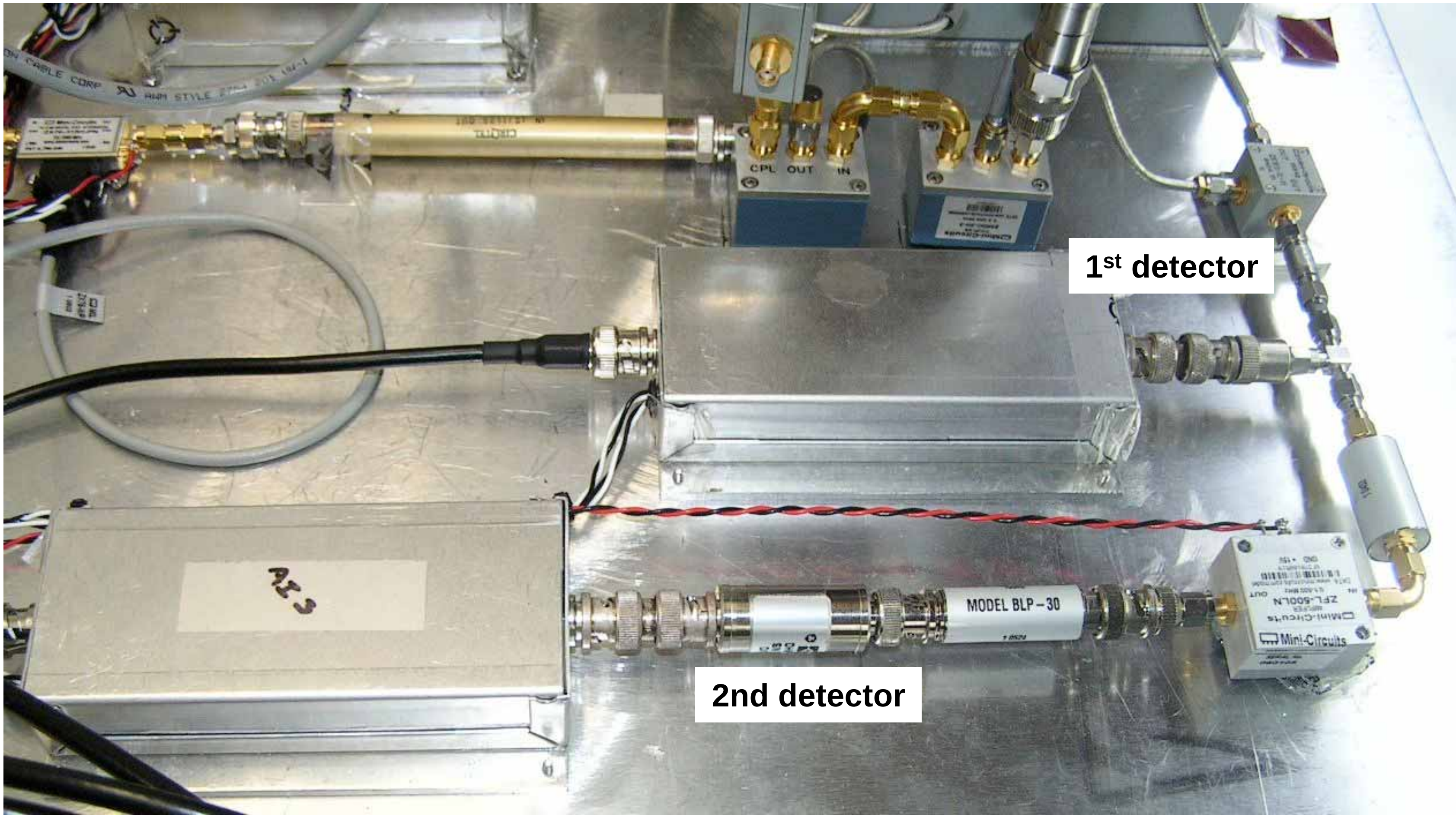

Linearize the Second Detector: Pseudo-Kurtosis

Non linear Kurtosis using absorber test

Linearized Kurtosis using absorber test

$$Kurtosis_{linearized} = \frac{moment_4}{moment_2^{\,2}} = 1$$

$$Kurtosis_{nonlinear} = \frac{v_2 - nulloffset}{(v_1 - nulloffset)^2}$$

- Results:
  - Find d_1-d_4
  - Find p.k. scale factor
  - Linearized p.k. = 1

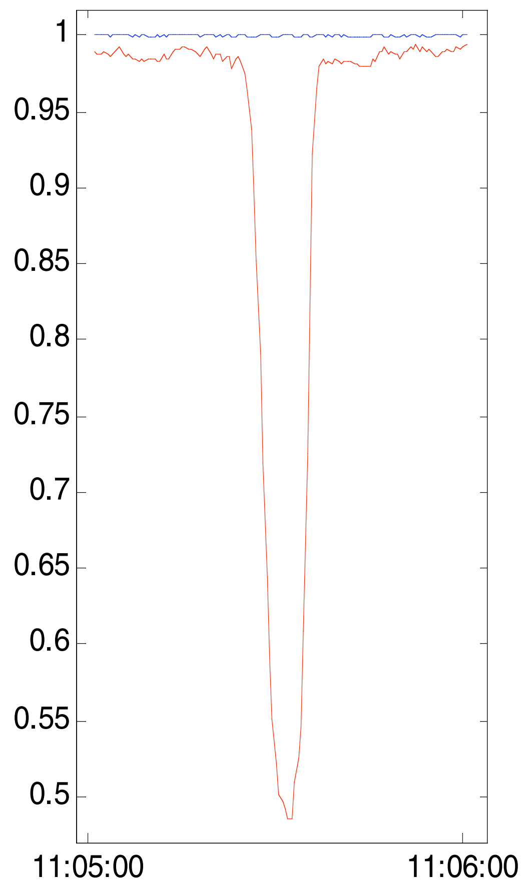

RFI Detected by GSFC Analog Double Detector Kurtosis during JPL PALS Campaign

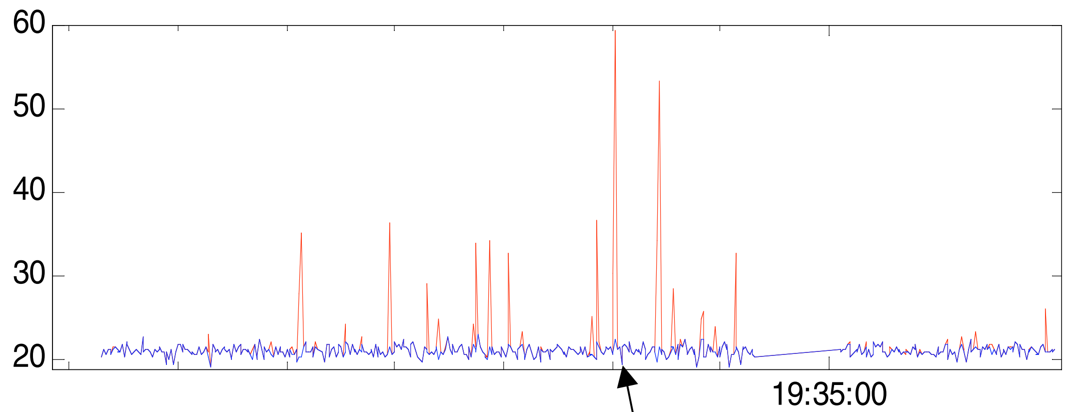

Pulse-blanked data

Un-blanked data

RFI not removed by blanking

Conclusions

- **Direct measurement of higher order moments (#1-4) can be used to reliably detect non-gaussian RFI; The signal kurtosis is a very robust statistic on which to base a detection algorithm**
- **Experimental verification of Δkurtosis noise floor**
  - **$\sigma_k = 0.005$ is consistent with $[24/(B\tau)]^{1/2}$ theory**
  - **3σ deviation is exceeded with RFI level ~ $2NE\Delta T$**
- **Digital subbands allow RFI to be removed**
- **No fundamental obstacles to use in spaceborne radiometers with currently available rad-hard space-qualified FPGAs**
- **Analog "Double Detector" architecture further reduces technology risk for flight design**